SLAC-TN-70-34
T. M. Jenkins,
G. J. Warren, and
J. L. Harris
December 1970

# Angular Distribution of Radiation From A Collimator, A Thick Plate and A Thin Plate Struck by a 2 GeV Electron Beam

## I. Introduction

It is common practice to use collimators as devices for preventing a beam from striking components such as magnets and vacuum flanges. Often, collimators are employed as personnel protection devices to prevent a beam from entering an area that may be occupied.[1] In this latter usage, the bremsstrahlung from the collimator itself must be shielded before an area is safe for personnel. This will require a knowledge of the angular distribution of the radiation emerging from the collimator.

Also, it is probable that a beam will target at small angles in a thick target such as a beam hitting the inside face of a magnet, or in a thin target, such as thin-walled aluminum transport pipe. A knowledge of the radiation pattern from each of these targets will allow one to calculate absorbed doses in magnets downstream of the source.

Another question that arises is: can radiation sources be localized (i.e., by using collimators) such that localized shielding may be employed only around the source itself, and not downstream? Considerable savings in cost and space would result if the answer were affirmative. However, to answer the question, the angular distribution of the emerging radiation must be known.

A series of tests were made at SLAC with a 2 GeV electron beam striking an iron plate, an iron collimator, and a thin aluminum plate with the resulting radiation pattern measured using thermoluminescent dosimeters (TLD) and ion chambers. The results of those tests are presented as a series of figures at the end of this report.

2. Experiment

A. General - A collimator may be struck at an entrance edge by a mis-steered beam, or it may be struck a glancing angle along an interior face. In both cases, the scattered radiation would be channeled in the forward direction with the sides of the collimator effectively shielding the larger angles, and with the forward angles, defined by the collimator opening, having the highest intensities. A second possibility is that a beam may strike an interior face near the downstream end, where the opposite face is no longer an effective shield except for extremely large angles.

The geometries are such that the problem does not lend itself to a simple model for calculation. For example, at small angles the radial thickness is changing as the electromagnetic shower develops.

The scattered radiation emerging from a thin plate, such as a beam transport pipe struck at small angles by an electron beam, is also of interest to the shielding designer. This case also is difficult because it lies between the thick and thin target geometries, with a variable radial thickness. The degree to which the electromagnetic shower develops is not known; consequently, the fraction of energy escaping the aluminum plate cannot readily be calculated. Yet this is a fairly probable occurence along beam transport systems.

B. Procedure - The electron energy, 2 GeV, was chosen to conform to the energy of the Stanford positron-electron asymmetric storage rings (SPEAR).[2] The collimator size, 3 feet in length with 5 inch thick walls, and a 3 inch square opening, was chosen to be typical of a collimator used in SPEAR. The thickness, 5", was chosen because it is the nominal thickness of the iron in the SPEAR bending magnets, and the results could be applied to the shielding of the ring itself. The iron plate was also 5" thick and 3' in length. The aluminum plate was $\frac{1}{4}$" thick, a nominal thickness for an aluminum transport pipe. Fig. 1 shows the three different geometries used in the experiment.

The experiment shown in Fig. 1(a) was divided into two parts. In the first part, $\phi$ was equal to $0^{\circ}$, and the beam steered into the 5" thickness of iron that made up one side of the collimator. Measurements downstream were made with the beam edge tangent to the inner edge of the iron, and also with the beam edge $\frac{1}{2}$ cm and $1\frac{1}{2}$ cm from the inner edge. In the second part, the collimator was pivoted to $3^{\circ}$ and $9^{\circ}$ with respect to the beam, and the beam steered to strike about halfway down one inner face.

Teflon capsules, about 1/8" in diameter, were filled with LiF (TLD) powder and placed on a wooden bench at a radius of 10' from the midpoint of the collimator. Angles from $-3^{\circ}$ to $+90^{\circ}$ were covered by the LiF capsules, with detectors every $1^{\circ}$ between $-3^{\circ}$ and $+5^{\circ}$, and at larger intervals beyond $5^{\circ}$. For the case where $\phi = 0^{\circ}$ in the first part, 1 mm diameter LiF rods spaced 2 mm apart were placed 10 feet downstream to cover the angles between -3 and +90 mradians.

In addition to the LiF dosimeters, two ionization chambers about 3/4 inch in diameter were placed 43 feet downstream. One chamber was fixed at $0^{\circ}$ while the other could traverse angles between 0 and 50 mradians.

Absolute beam intensities were measured to accuracies of a few percent using current toroids. Beam diameter, at the 10% intensity points as measured by darkening of glass plates, was 6.8 mm at the collimator location and 19 mm at the 43' downstream point for the experiment shown in Figure 1(a). For the experiments shown in Figures 1(b) and (c), the beam diameter was about 12 mm at the target. It was not measured downstream. Beam location was determined by viewing a ZnS screen at the entrance edge of the target. Beam steering was held constant, and the target (collimator or iron plate) pivoted to give different values for $\phi$. For the thin Al plate-Fig. 1(c)- $\phi$ was fixed at $4^{\circ}$.

## 3. Results

For the case of an electron beam striking a collimator, the collimator angle, $\phi$ , was rotated to $0^{\circ}$, $3^{\circ}$, and $9^{\circ}$, with scattered radiation measured between $-3^{\circ}$ and $+90^{\circ}$. The measured radiation is shown in Figure 2. The spike at $0^{\circ}$ for the incident angle, $\phi = 0^{\circ}$, was due to a part of the beam not striking the collimator. For this step of the experiment, the beam was targeted into the upbeam end of the collimator with the beam spot edge, as viewed on the ZnS screen, tangent to the inside edge of the collimator. Because part of the beam exists outside the spot diameter as seen on a ZnS, some of the beam could pass down the collimator hole without hitting anything.

The angle from the front edge of one face of the collimator to the rear edge of the opposite face was about $5^{\circ}$. As can be seen from Figure 2, for

$\phi = 0^{\circ}$, the intensity begins to drop at an angle, $\theta$, of about 5-6$^{\circ}$. Pivoting the collimator $\phi = 3^{\circ}$ would cause this drop-off to begin at about $\theta = 5 + 3 = 8^{\circ}$, which can be seen from Figure 2. Similarly, the $\phi = 9^{\circ}$ curve should begin dropping at about $\theta = 14^{\circ}$.

A considerable intensity of radiation can be seen at $\theta$ angles of less than 0$^{\circ}$. Calculations show this is not direct radiation, either muons or photons, coming through the 3 foot length of iron. Thus, using a collimator, there is no immediate drop-off at the exit edges.

Figure 3 shows in more detail the radiation pattern in the 0 to 75 mradian region for three different beam positions. In this measurement, the beam was targeted in the collimator face with the edge of the beam spot, 1) tangent to the inner face, 2) $\frac{1}{2}$ cm in from the inner face, and 3) $1\frac{1}{2}$ cm in from the inner face. For all three cases, $\phi$ was 0$^{\circ}$.

Figure 4 shows the measurements made with the beam striking a 5" thick iron plate 3 feet in length. See Figure 1(b). The plate was angled between $\phi = 1.5$ and 12$^{\circ}$ with respect to the beam. The absolute values on the negative side of $\theta = 0^{\circ}$ (the angles that are shadowed by the iron plate) are the same for $\theta = 3^{\circ}$ and 9$^{\circ}$ as those for the collimator measurement. We have no explanation for the humps between $\theta = 0$ and 3$^{\circ}$ (in the $\phi = 3^{\circ}$ and 9$^{\circ}$ cases), except to note that they cannot be caused by direct radiation from the beam passing through the plate.

Figure 5 shows the radiation measurements made with the electron beam traversing an aluminum plate at an angle $\phi = 4^{\circ}$.

## 4. Discussion

In Figures 2 and 4, $\phi$ is the relative angle between the collimator, or iron plate, and the incident beam. In this experiment, the collimator or plate was varied in order to change $\phi$, whereas in usual practice, collimators are fixed in position, and the beam angle changes. Thus, in the case of Figure 4, the position of the sharp rise in scattered radiation intensity is determined by the angle at which the plate was rotated. To use Figure 4 in a practical case where zero degrees is fixed, each curve should be shifted to the left by the amount of the plate rotation such that all curves show the sharp rise at zero degrees.

Figure 4 shows that there is a significant dose at any angle from a plate struck by a 2 GeV electron beam, and that the dose at all angles increases as the incident beam angle decreases. For shielding purposes, it must be assumed that a beam will strike at the worst angle, which is that closest to zero degrees. This situation is comparable to that in which the beam is allowed to target near to the downstream end of a collimator, where the opposite side of the collimator has little effect upon the scattered radiation. The situation is better at the larger angles if the beam can target only near the entrance face, which would produce the curves of Figure 2.

The large tail on the thin Al plate measurements cannot be explained by multiple scattering theory. The maximum longitudinal thickness traversed by the beam at an angle $\phi = 4^\circ$ is about one radiation length. This is still thin enough such that Molière scattering theory may be used. Fitting the scattering shape, which includes the finite beam shape, to the measured curve at $\theta = 0^\circ$, the intensity should be down to 1 rad-m$^2$/10$^{13}$ electrons at a scattering angle of less than 30°. This is clearly not the case. Also, summing the total number of electrons measured with the TLD, assuming 2 MeV/g/cm$^2$ per electron to convert from rads to electrons, gives a total number of electrons that is 10 times the number of electrons in the beam as measured on the current toroid.

The dose at large angles may be due to electrons generated in the shower process in the one radiation length of aluminum, or to delta rays, or both. The shower process is complicated due to the geometry of the target. We may, however, look at the energy of the $\delta$-rays and see if it seems reasonable.

The number, N, of $\delta$-rays, per incident electron, with energy greater than $W_{min}$ is given by integrating the Rutherford formula. This gives

$$N \cong 0.15 \frac{Z}{A\, W_{min}} \qquad \text{per g/cm}^2$$

with $W_{min}$ in MeV.

For one radiation length of aluminum ($X_o$ = 24.3 g/cm$^2$) and a measured N of 10 delta rays per incident electron, we have

$$10 = 0.15 \left(\frac{13}{27}\right) \frac{24.3}{W_{min}}$$

So $W_{min}$ = 0.18 MeV.

If, after one radiation length, we take shower multiplicity of electrons with $E \geq \epsilon_o = 40$ MeV (where $\epsilon_o$ is the critical energy) as about 4, then there are 4 high energy shower particles and 6 delta rays per incident electron at the measured location, and the ratio of delta rays/incident electron is 1.5. This increases $W_{min}$ to

$$W_{min} = \frac{1.8 \times 10}{1.5} = 1.2 \text{ MeV}$$

which is fairly low, but perhaps reasonable.

In calculating the dose that might be absorbed one meter away from a thin Al pipe struck at $4^o$ by a 2 GeV electron beam, the following assumptions might be made: 1) some fraction of the energy will escape the aluminum pipe, 2) the radiation will emerge with an angular dependence given in Figure 5. From this figure, it can be shown that the curve follows a $1/\theta^2$ dependence.

Then the dose in rads may be given by

$$D = W_o \frac{df}{d\Omega} \frac{1}{r^2} f \frac{1}{\lambda} C$$

where $W_o$ = incident total energy, $N_e E_o$

$\frac{df}{d\Omega}$ = angular distribution of the escaping radiation, $1/\theta^2$

$f$ = fraction of energy that escapes

$\lambda$ = effective absorption length of the scattered radiation in an object at 1 meter. For man, $\lambda \approx 30$ g/cm$^2$.

$C$ = conversion factor from eV to rads, $1.6 \times 10^{-8}$ rad - gm/MeV

If the curve is normalized at $\theta \approx 24^o$, the dose, $\frac{r^2 D}{N_e E_o}$ $\left(\frac{m^2\text{-rad}}{10^{13} e^- \text{- 2GeV}}\right)$, may be given by

$$\frac{r^2 D}{N_e \text{-} E_o} = k/\theta^2$$

where $k = 3.5 \times 10^4$ ( a constant which includes all the above terms).

For example, the dose calculated at $12^o$ would be 240 rads/$10^{13}e^-$ with the measured value being 220 rads/$10^{13}e^-$, and the dose at $60^o$ would be

9.6 rads/$10^{13}e^-$ with the measured value being about 11 rads/$10^{13}e^-$.

To compl-te the picture of radiation emerging from a thick target, Figure 6, from previous work at SLAC[3], shows the angular distribution of radiation from a 17 radiation length iron target that had a radial thickness of about 4 molière units. A molière unit is the characteristic measure for radial distributions in analytic shower theory, and is equal to $X_o E_s/\epsilon_o$, where $\epsilon_o$ is the critical energy of the material, and $E_s$ = 21.2 MeV. The intensity, at least in the forward direction, scales according to $e^{-\mu x}$, where $\mu$ is the minimum in the photon absorption coefficient, and is about 0.041 $cm^2/g$ for lead.

## R E F E R E N C E S


1. D. D. Busick, et al, "Beam Safety Considerations at the Stanford Linear Accelerator Center, SLAC-PUB-675 (1970).

2. B. Richter, The Stanford Positron-Electron Asymmetric Rings (SPEAR), SLAC-PUB-630 (1969).

3. The Stanford Two-Mile Accelerator, R. B. Neal, Editor, W. A. Benjamin, Inc. (1968).

## FIGURE CAPTIONS

Figure 1. Three different geometries used in experiment. Electron energy was 2 GeV for all three cases, a) thick collimator b) thick plate c) thin plate.

Figure 2. Scattered radiation from a beam striking the inner face of the collimator at beam angles, $\phi$ , of $0^{\circ}$, $3^{\circ}$ and $9^{\circ}$.

Figure 3. Scattered radiation in the forward direction for a beam striking the front face of a collimator at different distances from the inner surface. In all cases, $\phi = 0^{\circ}$.

Figure 4. Scattered radiation from a beam striking one edge of a thick iron plate at angles from $\phi = 1\frac{1}{2}^{\circ}$ to $12^{\circ}$. The spikes at $\theta \cong 3^{\circ}$ are not explained.

Figure 5. Scattered radiation from a beam striking a thin Al plate at an angle, $\phi = 4^{\circ}$.

Figure 6. Scattered radiation scaled for a 2 GeV electron beam striking a 17 $X_o$ iron target (From Reference 3).

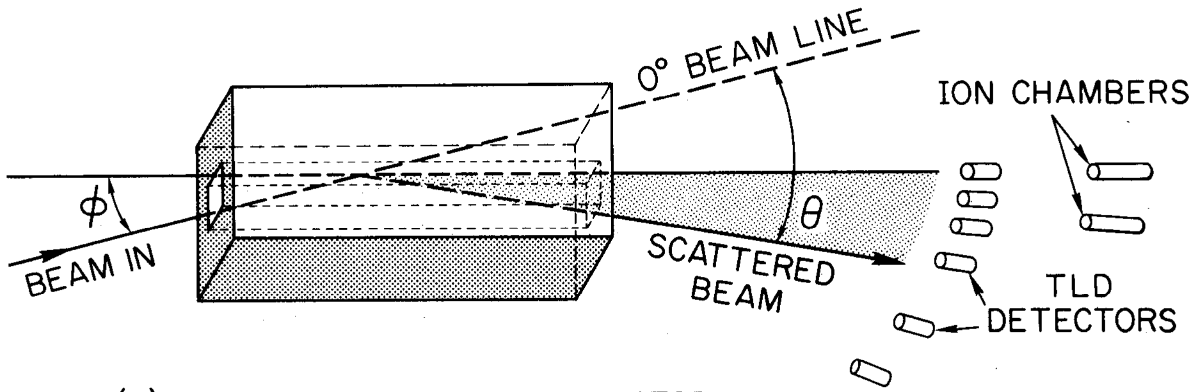


(a) SQUARE-HOLE IRON COLLIMATOR

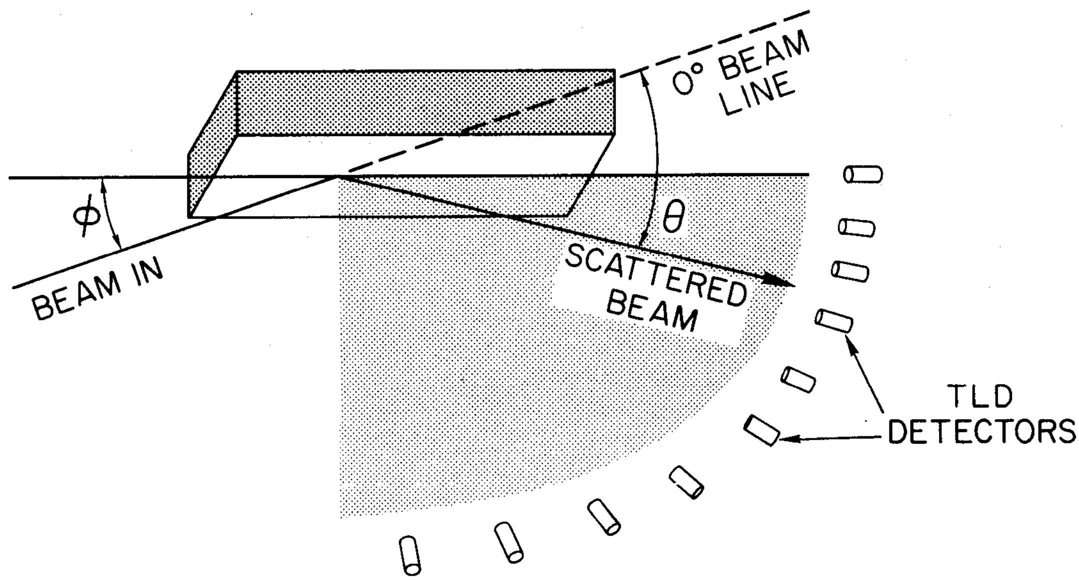


(b) THICK IRON PLATE

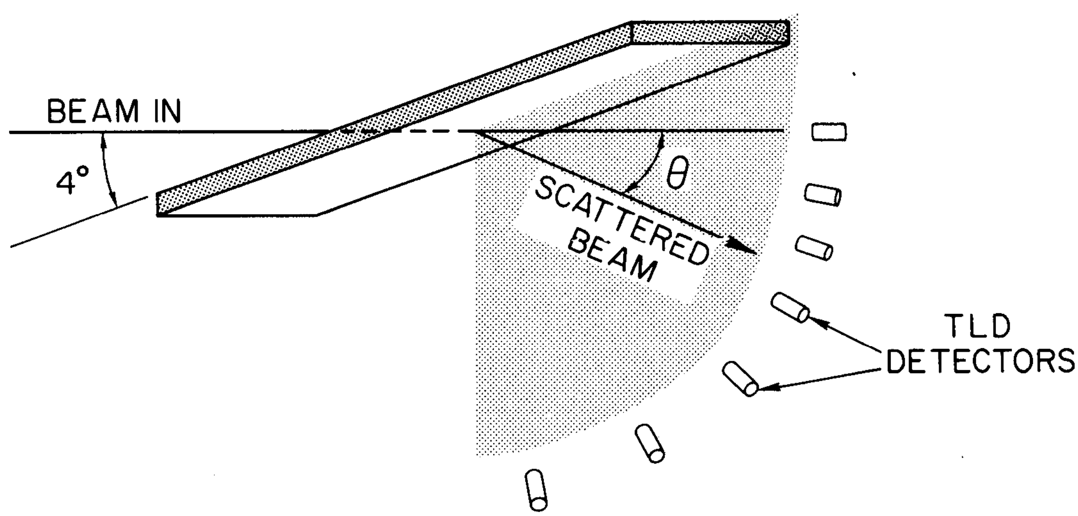


(c) THIN ALUMINUM PLATE

1714B4

Fig. 1

March 1971

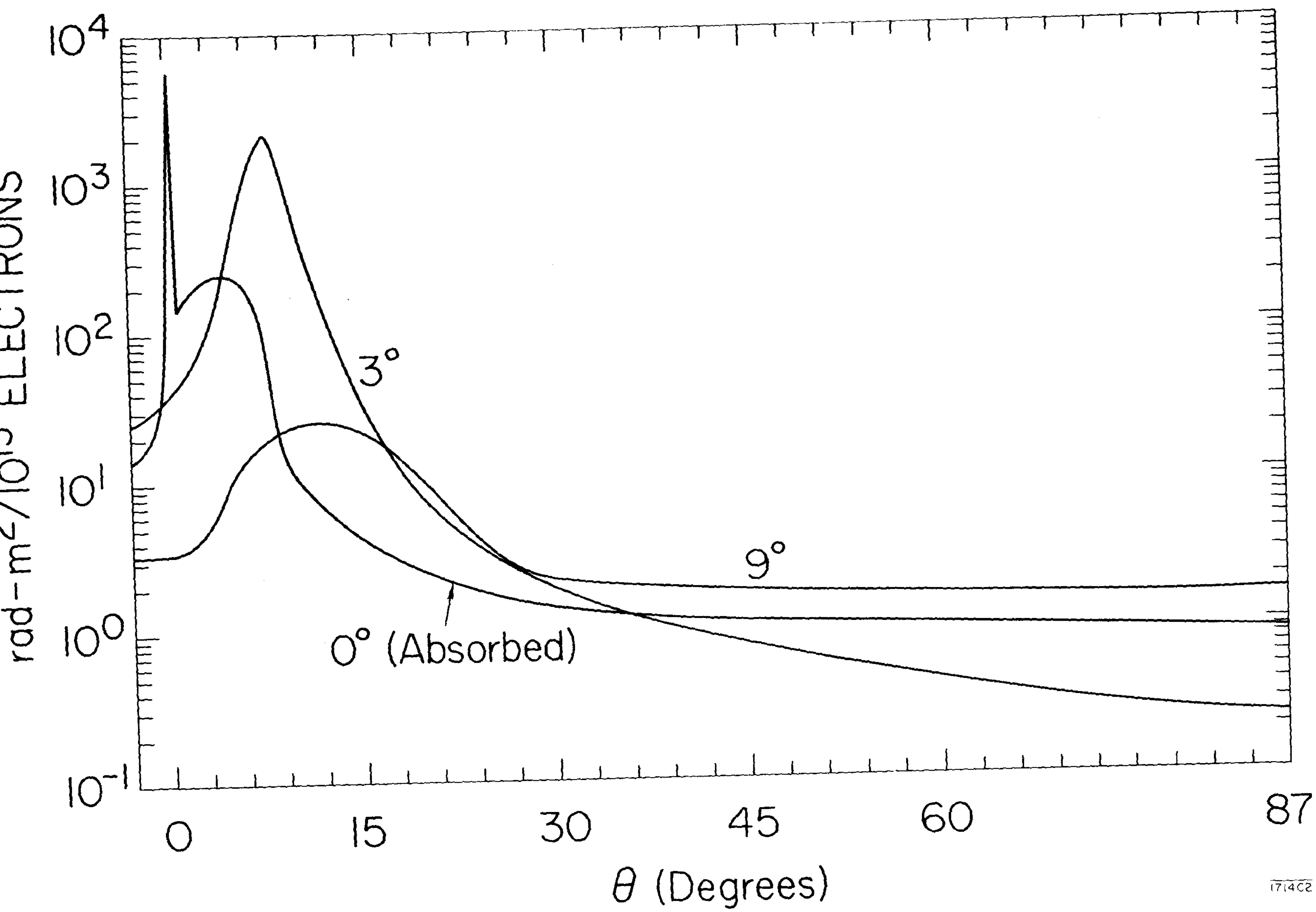

rad-m2/1013 ELECTRONS
104
103
102
101
100
10-1
3°
9°
0° (Absorbed)
0
15
30
45
60
87
θ (Degrees)
1714C2


Fig. 2

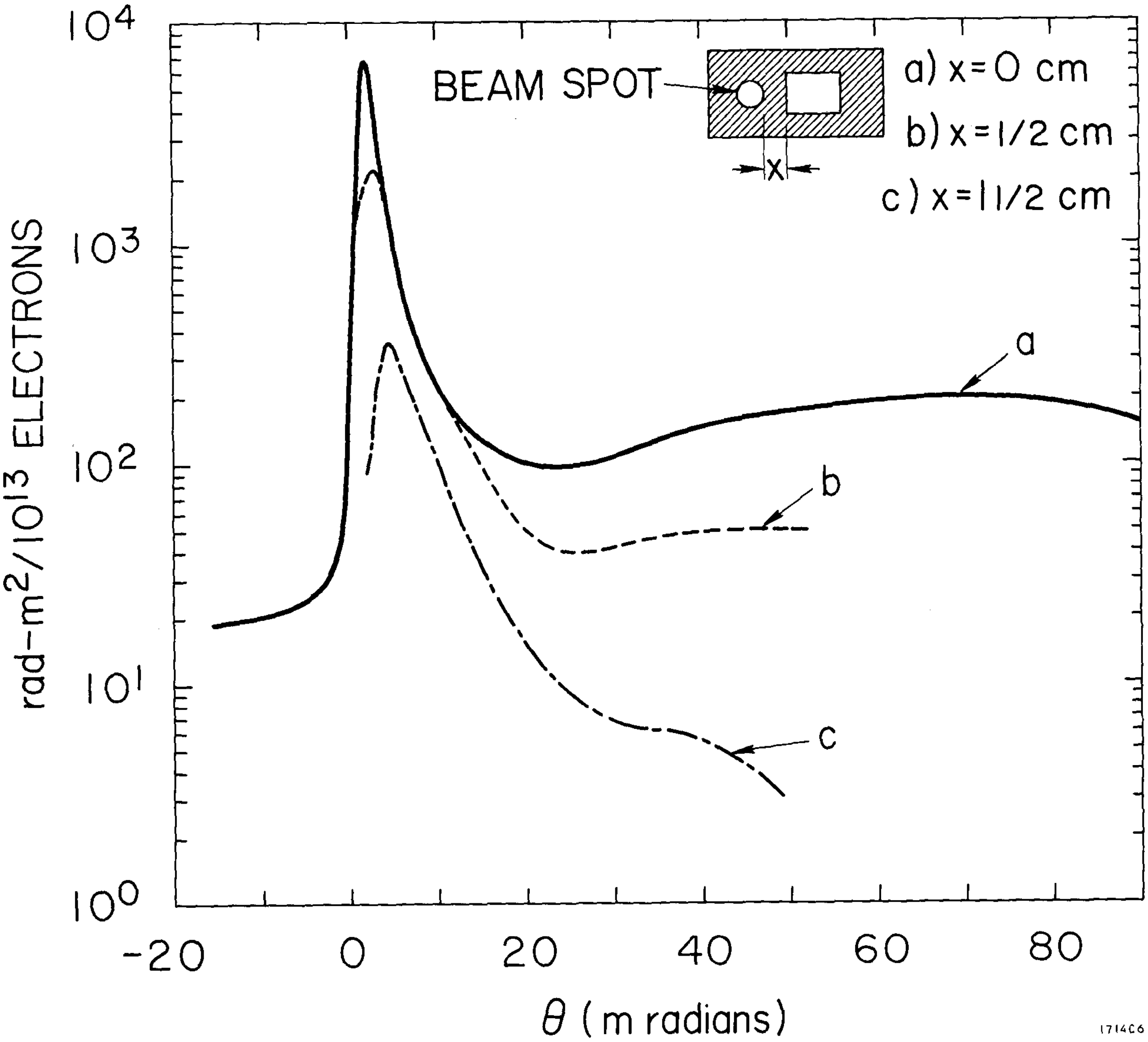

BEAM SPOT
x
a) x=0 cm
b) x=1/2 cm
c) x=11/2 cm
a
b
c
rad-m2/1013 ELECTRONS
θ (m radians)
171406


**Fig. 3**

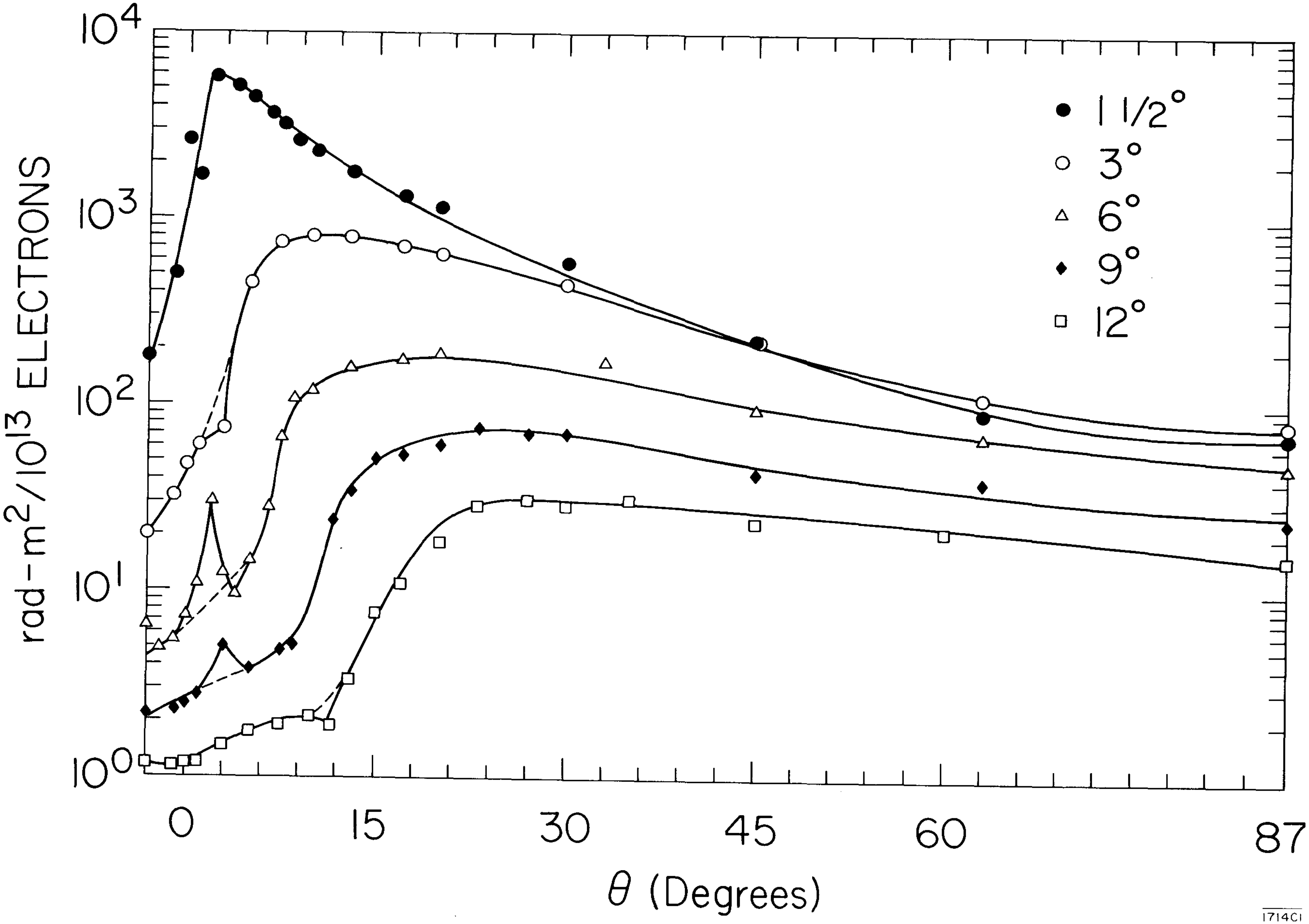

rad-m$^2$/10$^{13}$ ELECTRONS
$10^4$
$10^3$
$10^2$
$10^1$
$10^0$
0
15
30
45
60
87
$\theta$ (Degrees)
1 1/2°
3°
6°
9°
12°
1714C1


Fig. 4

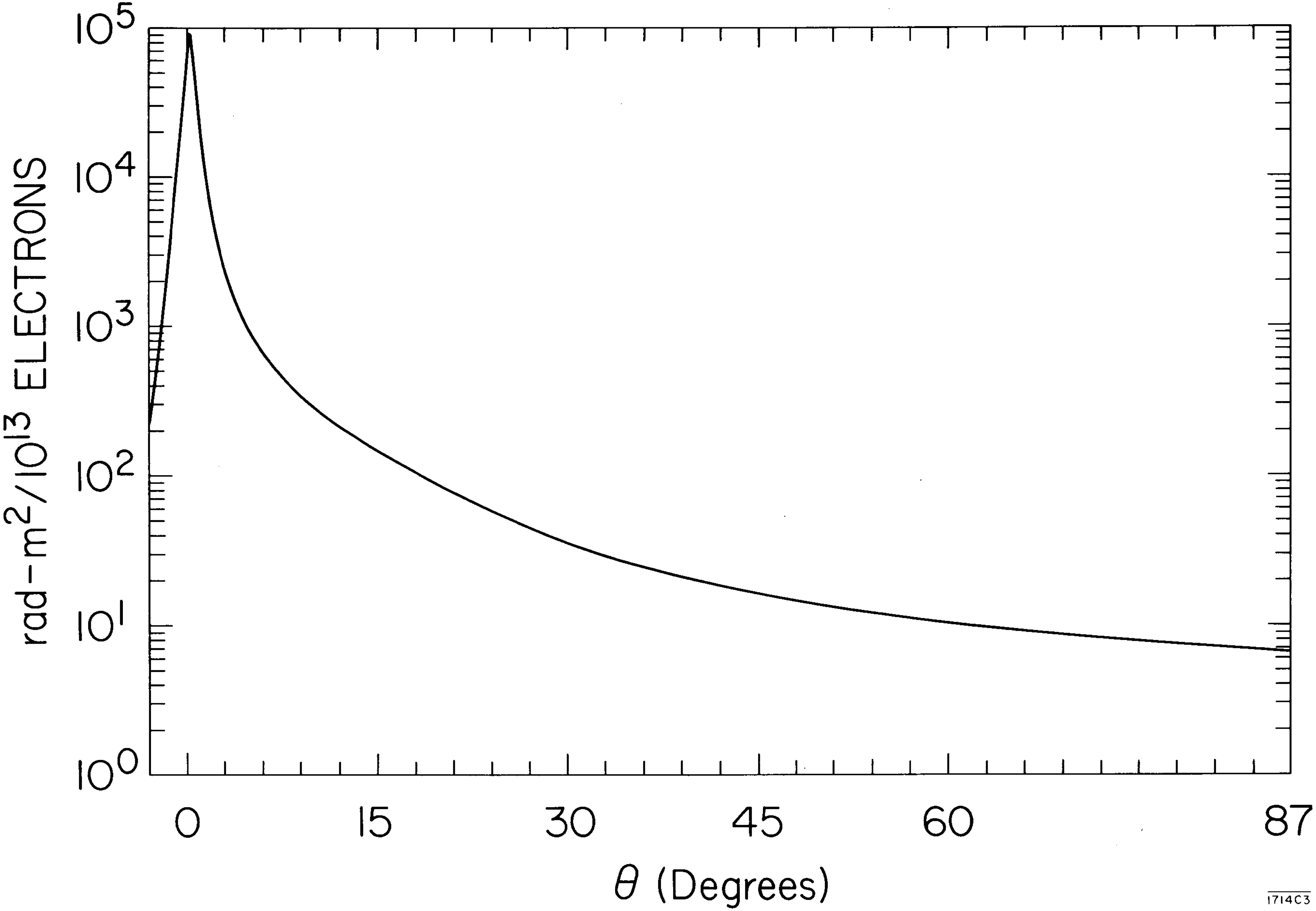

$10^5$
$10^4$
$10^3$
$10^2$
$10^1$
$10^0$
rad-m$^2$/$10^{13}$ ELECTRONS
0
15
30
45
60
87
$\theta$ (Degrees)
1714C3


Fig. 5

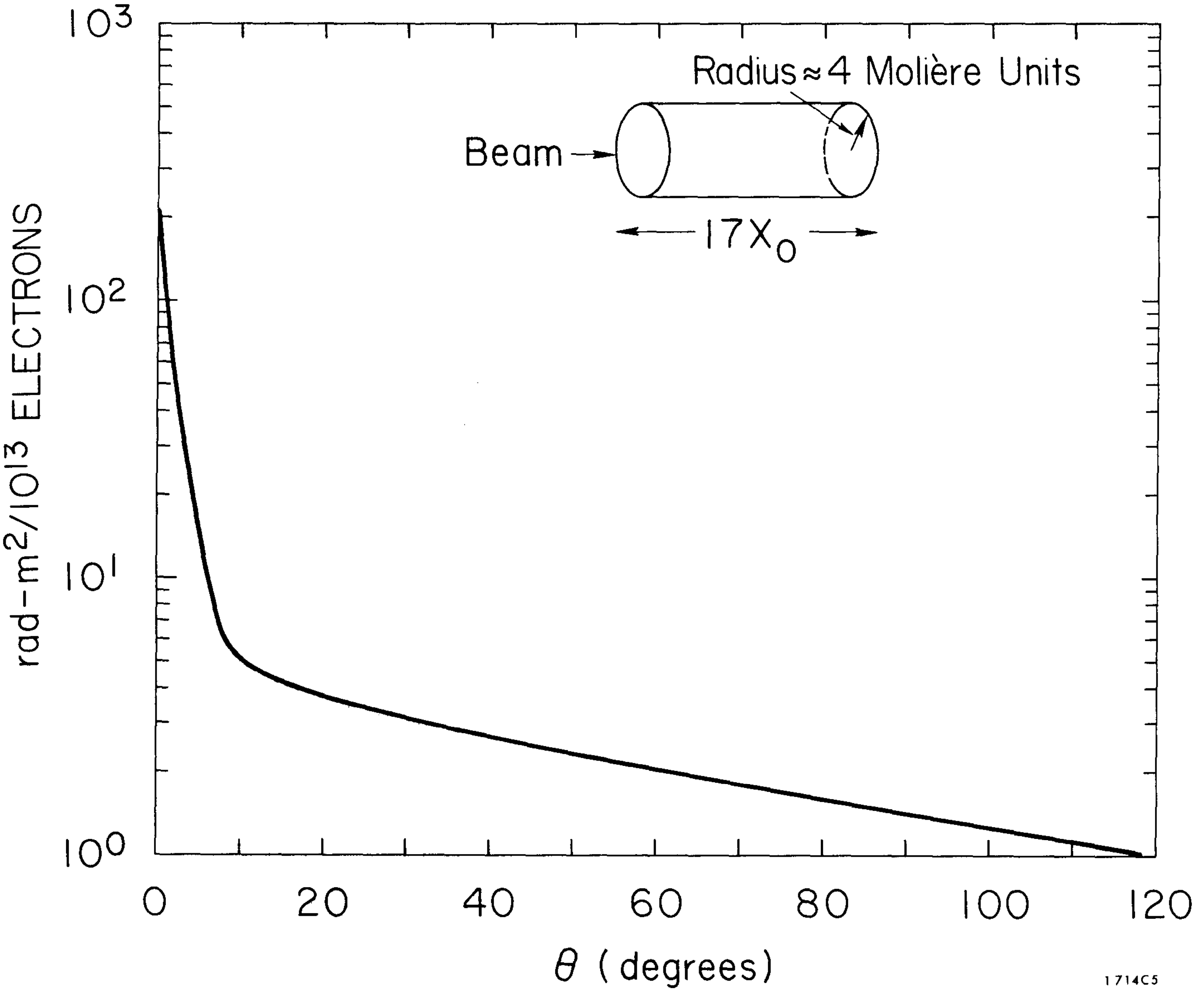

Radius ≈ 4 Molière Units
Beam
$17X_0$
rad-m$^2$/10$^{13}$ ELECTRONS
$10^3$
$10^2$
$10^1$
$10^0$
0
20
40
60
80
100
120
$\theta$ ( degrees)
1714C5


Fig. 6